Shap. Mem. Superelasticity (2019) 5:32–41
https://doi.org/10.1007/s40830-018-00202-5

SPECIAL ISSUE: HTSMA 2018, INVITED PAPER

Effect of Aging Heat Treatment on the High Cycle Fatigue Life of $Ni_{50.3}Ti_{29.7}Hf_{20}$ High-Temperature Shape Memory Alloy

Hasan H. Saygili[1,2] · H. Onat Tugrul[1] · Benat Kockar[1]

Published online: 7 December 2018

Abstract Shape memory alloys can be utilized as actuators for several applications in aerospace industry which require high strength and stable actuation cycles together with the transformation temperatures above 100 °C. Aging is one of the methods for Nickel rich NiTiHf alloys that adjusts the transformation temperatures and enhances the cyclic stability due to the formation of nano-sized precipitates. In this study, the high cycle functional fatigue life and behavior of the extruded and aged $Ni_{50.3}Ti_{29.7}Hf_{20}$ high-temperature shape memory alloy were investigated in order to reveal the effect of aging on the stability of the actuation strain and transformation temperatures. The aging was conducted at 550 °C for 3 h. 200 MPa was chosen in the functional fatigue experiments since no irrecoverable strain was determined under this stress magnitude for the extruded and the aged samples in the load-biased heating cooling experiments. The fatigue experiments were conducted twice to check the repeatability of the shape memory properties of the samples and it was observed that the life cycle of the aged sample was determined as 20,337 and the extruded sample completely lost the shape recovery ability after 5000 cycles.

Keywords Fatigue · NiTiHf · Shape memory · Aging

Introduction

Shape memory alloys (SMA) are very unique and special materials with the ability of remembering their original shape via heating after they have been deformed. This unique property of SMAs leads to use them as actuators. Their high power-to-weight ratio makes possible to utilize them in aerospace, medical, and automotive industries [1–5].

Many studies have been conducted on binary Ni–Ti SMAs, since they have good cyclic stability, high actuation strain, and mechanical properties [6–8]. However, their martensitic transformation temperatures are lower than 100 °C such that the usage of these materials are limited for most the applications. Recently, controlling the actuation behavior of SMAs at high temperatures has attracted a great attention. The SMAs which are utilized for high-temperature applications are categorized as "High-Temperature Shape Memory Alloys" (HTSMAs) if their transformation temperatures are above 100 °C.

It has been addressed in the literature that Au, Pt, Pd, Zr, and Hf are used as additional alloying elements in NiTi binary systems to increase their transformation temperatures [9–12]. However, Au, Pt, and Pd are not suitable for commercial applications since their costs are relatively higher than that of the others. Thus, studies are focused on Zr and Hf addition in last decades. High oxygen affinity and brittleness of Zr make Hf the most promising alloying element in NiTi systems [11–16].

In Ni-rich NiTiHf HTSMAs, nano-scale precipitates can be formed via aging. These nano-scale precipitates strengthen the matrix, so critical stress for slip increases.

This article is an invited paper selected from presentations at the 2nd International Conference on High Temperature Shape Memory Alloys and has been expanded from the original presentation. HTSMA 2018 was held in Irsee, Germany, May 15–18, 2018, and was organized by the German Materials Society (DGM).

✉ Benat Kockar
benat@hacettepe.edu.tr

[1] Department of Mechanical Engineering, Hacettepe University, Beytepe, 06800 Ankara, Turkey

[2] Turkish Aviation Industry, Rotary Wing Technology Center, Kahramankazan, 06980 Ankara, Turkey

This increase leads to the formation of less plastic deformation even when huge stress levels are applied [17]. Nano-scale precipitates have two distinct effects on transformation temperatures. First one is the increase of the transformation temperatures with the formation of the Ni-rich precipitates which leads to the decrease of the Ni-content in the matrix. The second one is the stress field around the nano-precipitates which leads to an increase in the undercooling for complete martensitic transformation and, thus, a decrease in the transformation temperatures is observed. Therefore, it can be concluded that precipitation size and amount are very important parameters for tailoring the transformation temperatures. $Ni_{50.3}Ti_{29.7}Hf_{20}$ (at%) HTSMA is one of the most widely studied HTSMAs, since the transformation temperatures can be adjusted precisely via precipitation hardening [14, 18]. In addition to that, high critical stress for slip via aging makes $Ni_{50.3}Ti_{29.7}Hf_{20}$ the most promising HTSMA [19]. Previous studies have shown that aging for 3 h below 500 °C leads to a decrease in transformation temperatures. However, aging for 3 h above 500 °C increases the transformation temperatures [19]. Additionally, aging $Ni_{50.3}Ti_{29.7}Hf_{20}$ alloy at 550 °C for 3 h gives optimum results in the literature if the magnitude of the transformation temperatures and cyclic stability behaviors are considered [18].

There are many studies on $Ni_{50.3}Ti_{29.7}Hf_{20}$ HTSMAs such as load-biased heating and cooling experiments, stress-free transformation behavior, and microstructural investigations [20]. However, effect of aging on the high cycle functional fatigue properties of $Ni_{50.3}Ti_{29.7}Hf_{20}$ HTSMAs has not been demonstrated yet. Only two studies on fatigue behavior of $Ni_{50.3}Ti_{29.7}Hf_{20}$ HTSMA were conducted and published by Karaman and his group [21, 22]. However, the main focus in their first study was to show the effect of upper cycle temperature (UCT) and in their latest study, they focused on the effect of applied stress level on the functional fatigue response of $Ni_{50.3}Ti_{29.7}Hf_{20}$ aged at 550 °C for 3 h.

On the other hand, this study is about showing the effect of aging on the $Ni_{50.3}Ti_{29.7}Hf_{20}$ HTSMA via following the aforementioned optimum aging parameters and comparing the functional fatigue behavior of the extruded and aged samples in terms of actuation strain and transformation temperature stability. Therefore, this study has an importance with being the first study which reveals the enhancement of functional fatigue life and behavior via aging the $Ni_{50.3}Ti_{29.7}Hf_{20}$ HTSMA. The upper cycle temperature was not considered and the samples were heated till the reverse transformation was completed. The samples were fatigue tested for twice to check the repeatability of the shape memory properties such as transformation temperatures and actuation strain values.

Experimental Procedures

High-purity elemental materials of Ni, Ti, and Hf were used to fabricate $Ni_{50.3}Ti_{29.7}Hf_{20}$ HTSMA via vacuum induction melting under high-purity argon atmosphere. The material was then hot extruded at 900 °C with an area reduction of 4:1 after it was sealed in mild steel can in order to decrease the friction between the extrusion die and the material and to minimize the oxidation during hot extrusion process. This condition is referred to as "Extruded" throughout the text. A part of the extruded billet was wrapped in tantalum foil, which was 25.4 μm in thickness to diminish the oxidation during aging heat treatment and aged in a vertical cylindrical furnace at 550 °C for 3 h under high-purity argon atmosphere. The aging heat treatments were ended with water quenching and this condition is going to be referred as "Aged" throughout the text. Only 550 °C-3 h of aging treatment was conducted since it was already shown in the literature that this aging treatment condition provides better results in terms of shape recovery in load-biased heating cooling experiments for $Ni_{50.3}Ti_{29.7}Hf_{20}$ HTSMA [20]. Dog bone-shaped tensile test samples which were used in load-biased heating–cooling and functional fatigue experiments with a gage length of 16.6 mm, a width of 2.25 mm, and a thickness of 1 mm were cut using wire electrical discharge machine (WEDM). Differential scanning calorimetry (DSC) and optical microscope (OM) specimens were cut via diamond saw precision cutter without applying load and at a very low speed to prevent inducing stress.

Stress-free transformation temperatures of both extruded and aged $Ni_{50.3}Ti_{29.7}Hf_{20}$ samples were measured using Perkin Elmer Differential Scanning Calorimetry (DSC) 800 before load-biased heating–cooling and fatigue experiments. $Ni_{50.3}Ti_{29.7}Hf_{20}$ alloy has been studied before and there are publications which are showing the transformation temperatures in the literature [14, 18]. However, it has been already known that the small compositional differences from batch to batch in shape memory alloys can lead to changes in the transformation properties. Therefore, DSC experiments were also conducted before mechanical experiments in this study. Additionally, the load-biased heating–cooling experiments were performed to determine the threshold stress level of the batch used in this study at which the first irrecoverable strain was observed. There is a publication which is showing the load-biased heating–cooling experiments on $Ni_{50.3}Ti_{29.7}Hf_{20}$ HTSMA, therefore, the results which were obtained in this study are not shown. However, it should be known that these experiments were conducted on extruded and aged samples by increasing the applied load with a magnitude of 100 MPa and the first irrecoverable strain was observed under

300 MPa in the extruded sample. Thus, the functional fatigue experiments were done under 200 MPa by using a custom-built functional fatigue test setup. Tensile samples were mounted to the grips which were attached to the aluminum sigma profile chassis. The dead weights were hanged to the bottom grip in order to generate constant stress on the tensile samples. The material was heated with the electric current passing through the sample, which was called Joule heating method. Programmable DC power supply's negative and positive poles were connected to the grips. Temperature was measured from the mid-sections of the gage length of the samples with the Optris CTlaser LTF-CF1 infrared thermometer. Tensile samples were coated with high-temperature black paint to set the emissivity value to a constant value. Cooling was performed using compressed air which was forced to the tensile sample using an air nozzle. A digital electro-pneumatic regulator was used to control the amount of air flow. Displacement was measured with a linear potentiometric displacement sensor (LPDS) and actuation strain was calculated by taking the difference between martensitic and austenitic strains. Measurement, control, and data acquisition were performed using the program scripted on National Instruments LabView Software. National Instruments USB-6003 data logger was utilized as an input device via taking the data from the sensors and as an output device to control the proportional valve. The lower cycle and the upper cycle temperatures and the heating/cooling rate were entered manually to the program. PI controller integrated to the program controlled the electrical current passing through the sample during heating and the amount of air compressed to the sample surface during cooling in order to achieve the desired heating/cooling rate. Temperature, displacement, and number of cycle data were stored to the computer.

Optical Microscope (OM) was utilized to observe the crack formation and transmission Electron Microscope (TEM) was used to investigate the twinning formation and the precipitates in the extruded and aged samples, respectively, to exhibit the sizes of the twins, the precipitates, and the oxides in the matrix. TEM samples were prepared via utilizing focused ion beam equipment for thinning the samples down to 10–20 nm.

Experimental Results

DSC Results

DSC experiments were conducted on extruded and aged samples for three cycles and the transformation curves are shown in Fig. 1 for comparison. The transformation temperatures which were drawn from all three cycles are presented in Table 1. M_f temperature decreased from 33 to 27 °C, while A_f temperature decreased from 110 to 103 °C at the end of the 3 stress-free cycles for the extruded sample. Besides these, M_s and A_s temperatures of the extruded sample exhibited similar decreasing trend with the cycles.

On the other hand, aged sample showed better cyclic stability during stress-free transformation temperature measurements than that of the extruded sample. The decrease in all transformation temperatures of the aged sample was between 2 and 3 °C at the end of the three cycles and this indicates a better cyclic stability in terms of transformation temperatures, as expected. Likewise, transformation temperatures were above the threshold value which is 100 °C for satisfying the condition of being HTSMA.

Functional Fatigue Experiment Results

Functional fatigue experiments were conducted under constant stress magnitude of 200 MPa since irrecoverable strain was first observed under 300 MPa in load-biased heating–cooling experiment for the extruded sample as stated in the previous section. Therefore, 200 MPa stress magnitude was set as the threshold stress level for the high cycle fatigue tests. It has been already known that UCT decreases the functional fatigue life of HTSMAs [21]. Karaman and his group showed that actuation strain of the sample increases with the increase in UCT since there are some local regions where heating to higher temperatures is necessary for further transformation of martensite to austenite [21]. This increase in UCT results full transformation along the sample where increase in actuation strain accompanies it. Increase in actuation strain leads more expansion and contraction of cracks which promotes crack propagation [21]. Other effect of UCT can be considered as decreasing the strength of the material with the increase in temperature, which results early failure. UCT level is critical for fatigue life determination; however, in this study, UCTs were set to 130 °C above the A_f temperatures of the extruded and the aged samples which were found from the DSC experiments. $A_f + 130$ °C was chosen as the UCT temperature for all the cycles since the transformation temperatures shifted to higher temperatures with the number of cycles such that the complete transformation was achieved through all the cycles. Additionally, fatigue experiments were conducted on extruded and aged samples for twice to control the repeatability of the experiments and the fatigue behavior of the alloy.

Strain versus temperature responses from the repeated fatigue experiments of the extruded and the aged samples for the selected cycles are presented in Fig. 2a and b and Fig. 3a and b, respectively. It can be seen from Fig. 2a and

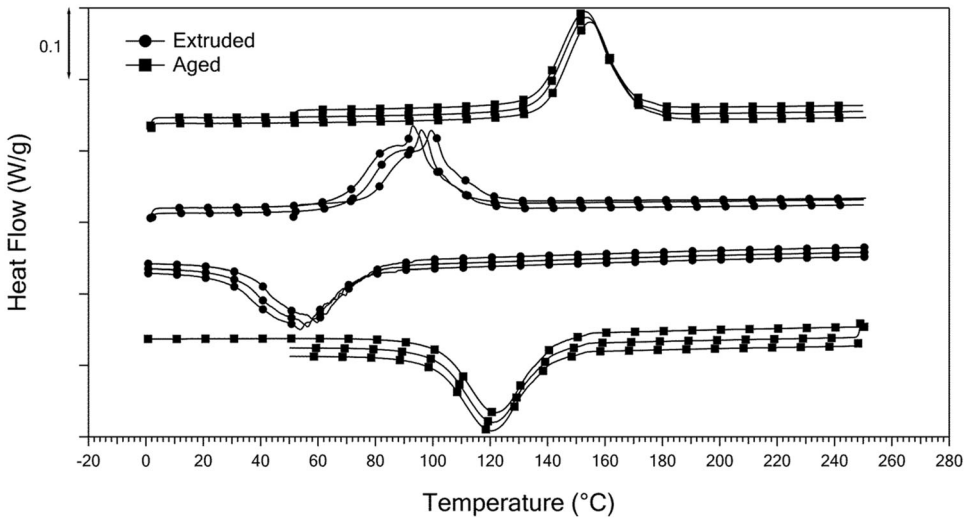

Fig. 1 Third cycle DSC curves of the extruded and the aged $Ni_{50.3}Ti_{29.7}Hf_{20}$ samples for comparison

Table 1 Transformation temperatures which were calculated from the DSC curves of the extruded and the aged $Ni_{50.3}Ti_{29.7}Hf_{20}$ samples

Sample	Cycle	Transformation temperatures (°C)			
		M_f	M_s	A_s	A_f
Extruded	1	33	80	77	110
	2	30	78	70	107
	3	27	75	67	104
Aged	1	101	142	138	171
	2	100	141	136	169
	3	99	140	135	168

b that the extruded sample completely lost the shape memory behavior after 5000 cycles in both of the experiments and the aged sample failed at 16,534th cycle in the first and at 20,337th cycle in the second experiment. There is a difference in the number of cycles between the first and the second experiment due to the possibility of having different amount of microcracks before starting the fatigue experiments. It can be noticed from Figs. 2 and 3 that, the functional fatigue life of the alloy was increased more than three times with the aging heat treatment.

Figure 4a and b represents the evolution of the transformation temperatures of the extruded and the aged samples with the number of cycles, respectively. All the temperatures were drawn from the strain versus temperature curves of the first and second fatigue experiments. The procedure to determine M_s, M_f, A_s, A_f temperatures and the actuation strain is shown on the 1st cycle curve in Fig. 2a.

It was seen from Fig. 2a and b that the transformation temperatures of the extruded sample were not possible to be determined after 1000th cycle since the transformation curves became very shallow. Figure 4a is drawn to compare the transformation temperature evolutions of the aged and extruded samples for the first 1000 cycles. Additionally, Table 2 is given to show the transformation temperatures of the extruded and the aged samples which were drawn from the 1st and 1000th cycles and the differences between them for better comparison. It can be easily seen that there is a noticeable decrease in the differences after aging heat treatment which is showing the effect of aging on the cyclic stability of the alloy under stress. On the other hand, all the transformation temperatures of the aged sample and A_s and M_f temperatures of the extruded sample showed a decreasing tendency on the order of 5 °C for the initial 100 cycles. The shift of the transformation temperatures of the aged sample up to 1000 cycles is less than that of the extruded sample and this can be drawn from the differences of the transformation temperature values which were shown in Table 2. Moreover, all the TTs of the aged sample showed an increasing tendency after 1000 cycles as it can be seen from Fig. 4b. Figure 5 demonstrates the actuation strain with the number of cycles of the extruded and the aged samples. The main observations from Fig. 5 can be summarized as follows:

(1) There is almost no difference in between the actuation strain values obtained from the first and second fatigue experiments of the extruded and aged samples, hence it can be concluded that the cyclic behavior of both of the samples is repeatable.
(2) Actuation strain values of the extruded sample started to decrease with a considerable amount from the beginning till the end of the 3000 cycles and almost no actuation strain was observed after 5000 cycles such that the experiments were stopped.
(3) Actuation strain values of the aged sample decreased with the number of cycles from 2.4% down to 1.7% in both of the experiments.

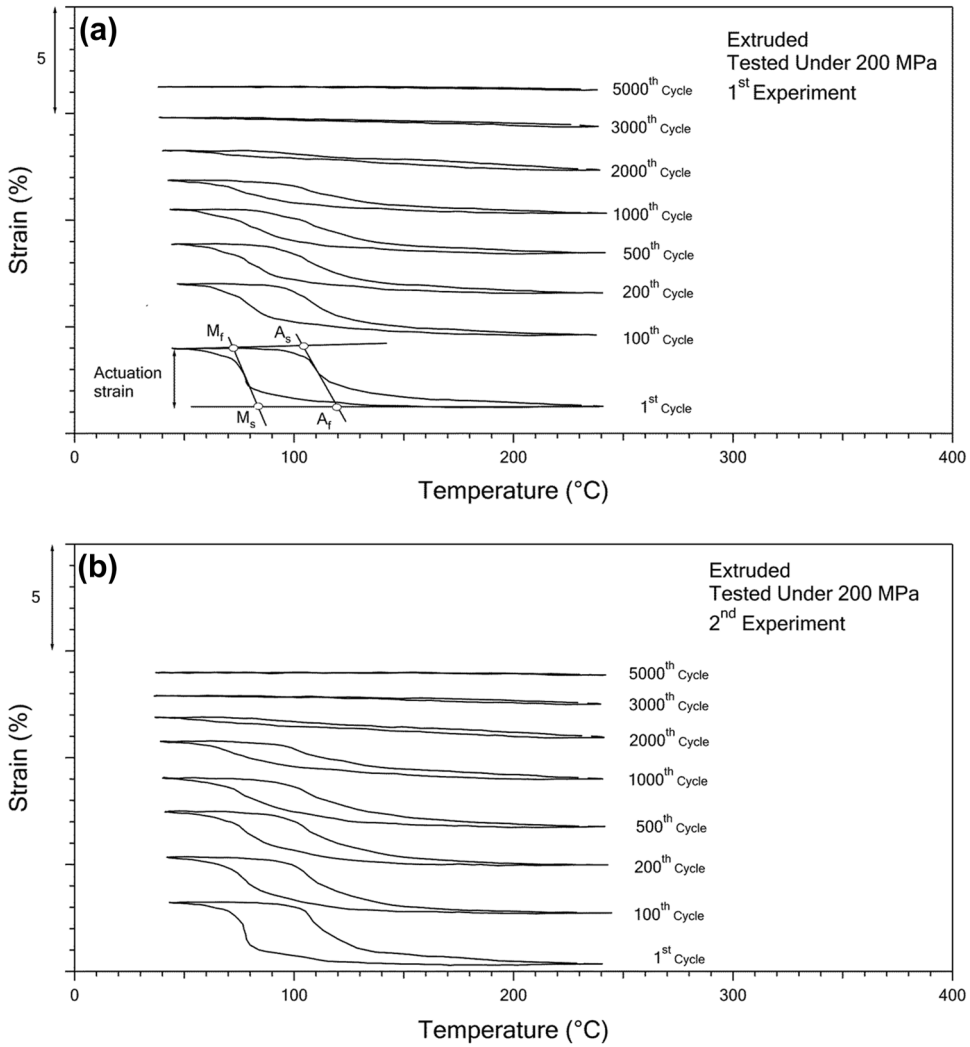

Fig. 2 Strain vs. temperature curves of fatigue tested extruded $Ni_{50.3}Ti_{29.7}Hf_{20}$ samples under 200 MPa **a** 1st experiment **b** 2nd experiment

(4) The actuation strain values of the aged sample were lower than that of the extruded sample at the beginning.
(5) There was a huge decrease in actuation strain values of the extruded sample, while the aged sample showed a very small change in actuation strain especially during the first 1000 cycles.

Microstructural Investigation

Optical Microscopy Results After Functional Fatigue Experiments

Figure 6 shows the optical microscope images of the extruded and the aged samples after the first functional fatigue tests. Microcracks were observed in both of the samples but the cracks of the extruded sample were smaller than that of the aged one. It is possible that cracks did not propagate since the extruded sample lost its shape recovery ability and the experiment was stopped. However, the aged sample was cycled for 16,534 cycles such that the higher number of cycles led to the propagation of cracks and to the fracture of the sample. Most of the cracks were initiated from the side surfaces of the samples.

Transmission Electron Microscope Studies

Transmission Electron Microscopy studies were also conducted to reveal the twin structure in the extruded and the precipitate formation in the aged samples. A common internal twin formation was observed and presented in Fig. 7a and no nano-sized precipitates were detected in the extruded sample and shown in Fig. 7b.

TiNiHf Oxide and Hf Oxide formations were also determined in the samples and the oxide particles in the extruded sample are shown in Fig. 8a and b. These particles were not equally distributed. They were most probably formed during solidification of the alloy since oxygen affinity of especially Hf element is very high such that

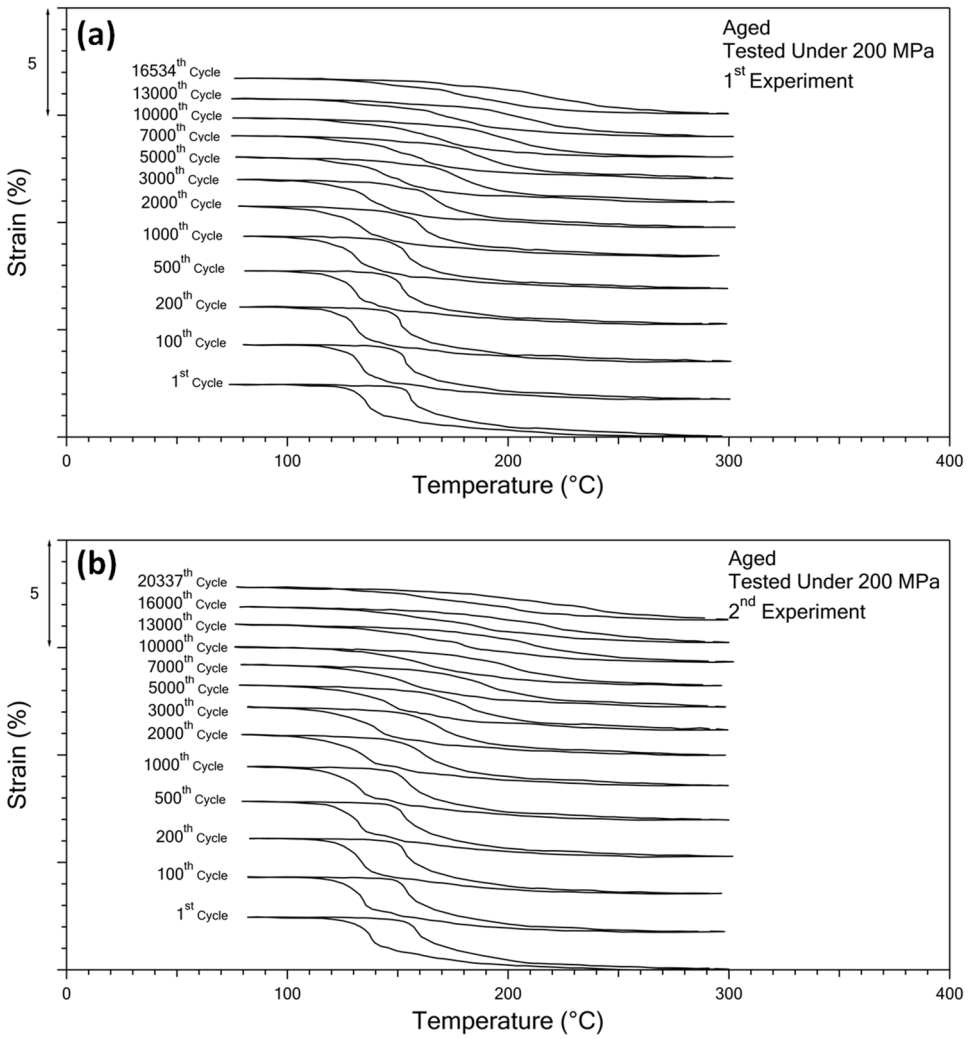

Fig. 3 Strain vs. temperature curves of fatigue tested aged $Ni_{50.3}Ti_{29.7}Hf_{20}$ samples under 200 MPa **a** 1st experiment **b** 2nd experiment

there is almost impossible to disallow the formation of the oxide particles in the matrix of TiNiHf alloys. The Energy-Dispersive Spectroscopy (EDX) Analysis of the precipitates in Figure 8a and b are given in Table 3a and b, respectively. It can be drawn from these compositions that the precipitate in Fig. 8a is a TiNiHf(O) and in Fig. 8b is a HfO types of precipitates.

Discussion of the Results

Aging Effect on the Stability of the Transformation Temperatures of $Ni_{50.3}Ti_{29.7}Hf_{20}$ Alloy with the Number of Cycles

There is a noticeable decrease in transformation temperatures of the extruded sample and this decrease is higher than that of the aged sample such that the thermal stability of the alloy increases with the aging heat treatment. The decreasing tendency of the transformation temperatures which was especially observed in the extruded sample with the number of thermal cycles in the DSC experiment is due to the introduction of the dislocations during the phase transformation [23]. Many studies have been conducted and published on the stability of transformation temperatures (TTs) of $Ni_{50.3}Ti_{29.7}Hf_{20}$ using DSC in the literature and it has been shown that the stability of TTs increases after aging the alloy at different temperatures for different time periods due to the formation of nano-sized precipitates [14, 18]. Additionally, it has been already known that, if the aging temperature is lower than 450 °C, a decrease in the transformation temperatures is observed due to the formation of very small precipitates such that additional undercooling is necessary. However, if the aging temperature is higher than 500 °C the chemical composition effect becomes dominant such that the Ni-content in the matrix decreases and the transformation temperatures increase. All the DSC results in this study are very well comparable with the results in the literature.

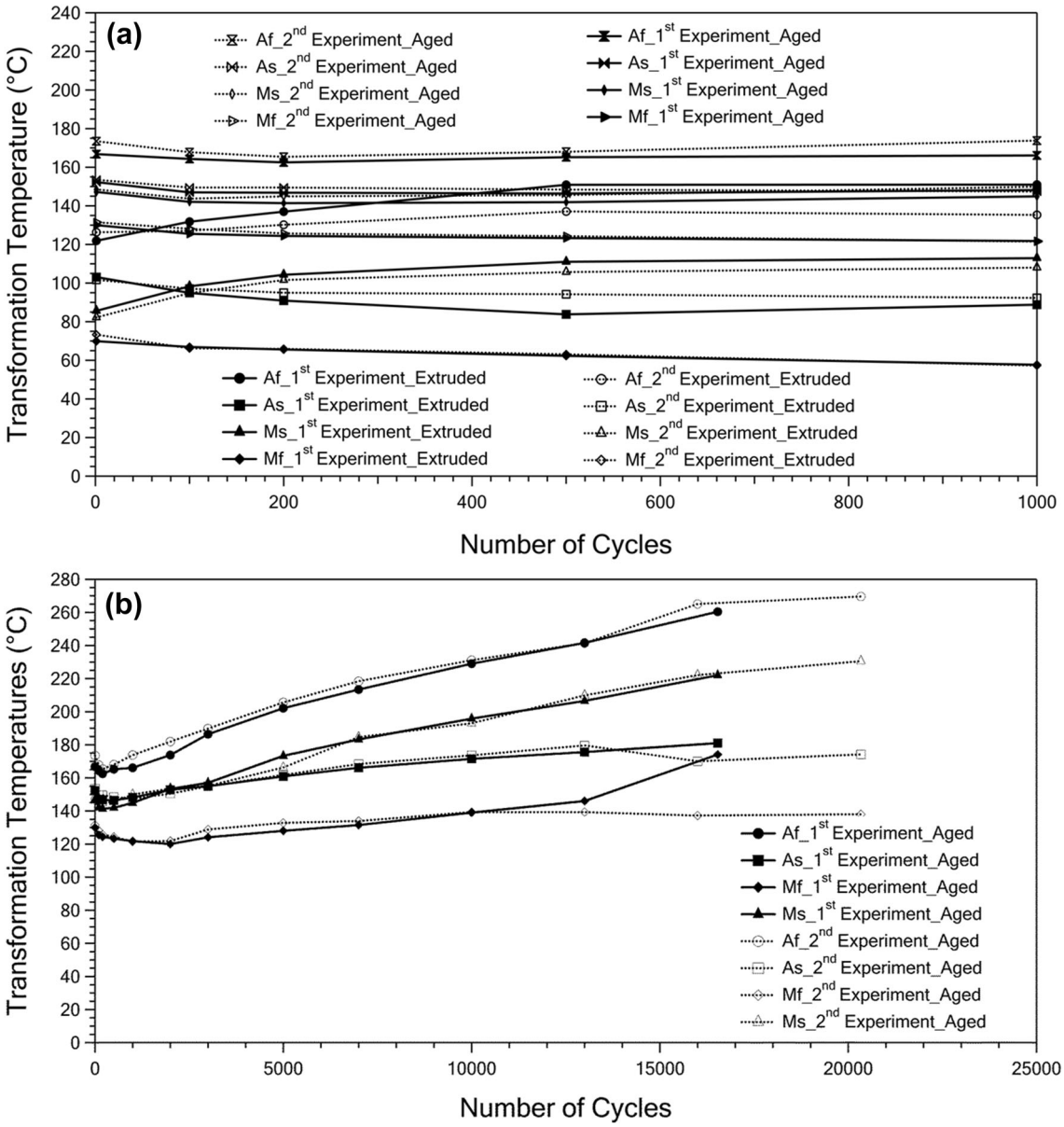

Fig. 4 Transformation temperatures which were drawn from the 1st and 2nd fatigue experiments of **a** extruded and aged $Ni_{50.3}Ti_{29.7}Hf_{20}$ samples for the first 1000 cycles and **b** aged $Ni_{50.3}Ti_{29.7}Hf_{20}$ sample

Table 2 The transformation temperatures of the extruded and aged $Ni_{50.3}Ti_{29.7}Hf_{20}$ samples which were drawn from the 1st and 1000th cycle strain versus temperatures curves of the first fatigue experiments and the differences of the temperatures

	M_f		M_s		A_s		A_f	
	1st	1000th	1st	1000th	1st	1000th	1st	1000th
Temperature (°C)								
Extruded	70	58	86	113	103	89	122	151
Aged	130	122	147	157	152	148	167	166
Difference (°C) (1^{st}–1000th)								
Extruded	− 12		27		− 14		30	
Aged	− 8		10		− 4		− 1	

The main focus of this study is to investigate the effect of aging on the high cycle functional fatigue behavior of $Ni_{50.3}Ti_{29.7}Hf_{20}$ alloy under constant stress. Therefore, the attention should be paid to Fig. 4 and Table 2. There is a

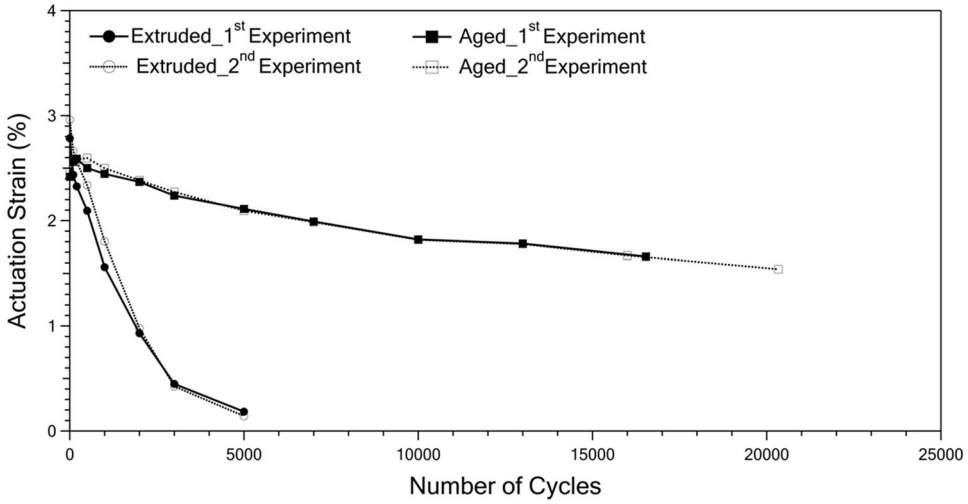

Fig. 5 Actuation strain values from the first and the second experiments with the number of cycles which were drawn from the curves of functional fatigue experiments of the extruded and the aged $Ni_{50.3}Ti_{29.7}Hf_{20}$ samples

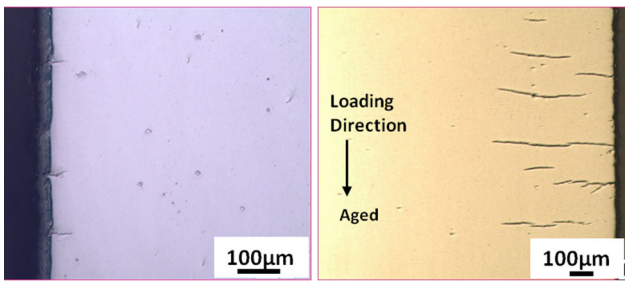

Fig. 6 Optical microscope images showing the crack formation in **a** the extruded and **b** the aged $Ni_{50.3}Ti_{29.7}Hf_{20}$ samples which were fatigue tested

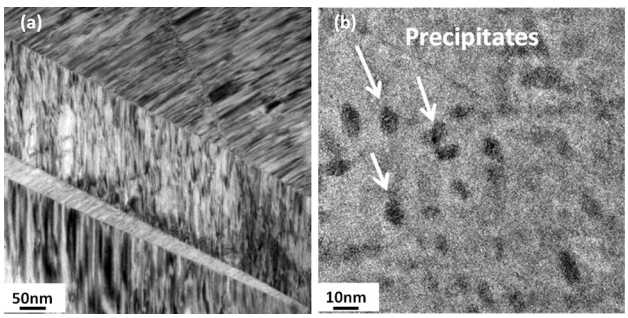

Fig. 7 TEM images of **a** the extruded $Ni_{50.3}Ti_{29.7}Hf_{20}$ sample showing internal twins **b** the aged $Ni_{50.3}Ti_{29.7}Hf_{20}$ sample with nano-sized precipitates

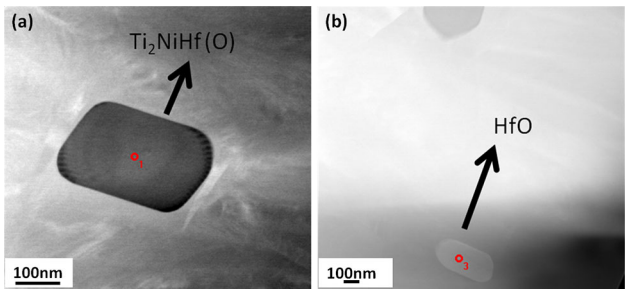

Fig. 8 TEM images of the $Ni_{50.3}Ti_{29.7}Hf_{20}$ extruded sample showing **a** TiNiHf(O), **b** HfO precipitates

Table 3 Energy-dispersive spectroscopy analysis of the precipitates in **a** Fig. 8a and **b** Fig. 8b

Element	Atomic %
(a)	
O	13.42
Ti	38.95
Ni	27.44
Hf	20.18
(b)	
O	65.97
Ti	0
Ni	0
Hf	34.03

decrease in the transformation temperatures of the aged sample on the order of 5 °C during the first 100 cycles since 200 MPa stress magnitude might not be enough for the strengthened sample via aging to induce high internal stress to form aligned martensite variants. However, it is obvious that aging has a positive effect on the thermal stability of the alloy if the first 1000 cycles are considered. The shift of the transformation temperatures was determined as the difference of the temperatures between the 1000th and the 1st cycles of the fatigue experiments and presented in Table 2 as mentioned before. A_f and A_s temperatures of the aged sample stayed almost constant during first 1000 cycles and the decrease in the M_f and the increase in the M_s temperatures were found as 8 and 10 °C, respectively. On the other hand, the differences of the transformation temperatures between the 1000th cycle and the 1st cycle of the extruded sample varied approximately between 12 and 30 °C. The noticeable increase in the M_s and A_f temperatures of the extruded sample under 200 MPa with the number of cycles can be attributed to the

increase in dislocation density in the absence of nano-sized precipitates with the number of cycles. Also, M_f and A_s temperatures of the extruded sample decreased 12 to 14 °C during 1000 cycles which might be again due to the increased internal stress associated with the increase in the number of dislocations. Additionally, the transformation temperatures of the aged sample also increased through the end of the fatigue experiment because the extensive thermal cycling under stress leads to increase in the internal stress associated with the formation of oriented martensite variants [24]. Therefore, it would not be legitimate to think that the full stability of the transformation temperatures can be maintained even in the aged condition. In the literature, the thermo-mechanical cycles which were conducted on the shape memory alloys were restricted to lower numbers. It should be noted that only the studies which were conducted by Karaman's group showed high number of cycles in fatigue experiments.

Aging Effect on the Actuation Strain Evolution and the Functional Fatigue Life of $Ni_{50.3}Ti_{29.7}Hf_{20}$ Alloy

To understand the effect of aging on the actuation strain values in the functional fatigue experiments, Fig. 5 was shown to compare the actuation strain evolution of the extruded and the aged samples with the number of cycles. Higher actuation strain values were attained from the extruded sample at the beginning of the fatigue experiment; however, a sharp decrease in the actuation strain values was observed since there was no barrier to the dislocation motion during the cycles. Additionally, the extruded sample lost all its shape recoverability at the end of the 5000th cycle. This can be attributed to the effective increase in the dislocation density of the extruded sample such that the dislocations lock the martensite-austenite boundary movement which is necessary for phase transformation and 200 MPa stress magnitude is not enough to overcome this mobility issue. Moreover, it was not possible to determine the transformation temperatures of the extruded sample after 1000 cycles since the strain–temperature curves which were obtained from functional fatigue experiment became very shallow.

Nano-sized precipitate formation with aging at 550 °C for 3 h increased the strength of the $Ni_{50.3}Ti_{29.7}Hf_{20}$ which led to the decrease in actuation strain values at the beginning but to increase the stability of the actuation strain with the number of cycles. The difference between the first and the last values of the actuation strain of the aged sample is 0.7%. Please note that, more than 16,000 cycles were run on the aged sample. There was almost no change in the actuation strain value of the aged sample throughout the first 1000 cycles. Therefore, it was better to compare the cyclic stability of the aged sample with the cyclic stability of the extruded sample considering the initial 1000 cycles. It is clear that the nano-scale precipitates increased not only the stability of the transformation temperatures but also the actuation strain values of $Ni_{50.3}Ti_{29.7}Hf_{20}$.

Aging heat treatment also significantly increased the fatigue life of the $Ni_{50.3}Ti_{29.7}Hf_{20}$ alloy. Dislocation accumulation in the aged sample was very much less than that of the extruded sample especially through the first 1000 cycles due to precipitate formation during the aging heat treatment. However, dislocation formation cannot be totally prohibited as the number of cycles increase and these dislocations led to initiation of the cracks. The crack density was increased with the initiation and propagation of the cracks especially at high temperatures such that the aged sample fractured at the end of 16,534th cycle in the first and 20,337th cycle in the second experiment.

One another reason to observe fracture can be due to the fact that HfO and TiNiHfO particle formation can act as the crack initiation points. These particles which were observed by TEM studies can cause relatively early failure. However, oxide particles mostly form during the solidification process such that the decrease in fatigue life should be expected for both the extruded and the aged samples. Thus, oxide particle formation was not enough to explain the difference of fatigue life for the extruded and the aged samples.

Conclusion

It has been already known that the nano-sized precipitate formation in NiTiHf alloys with the aging heat treatments increases the matrix strength and the cyclic stability of the transformation temperatures without applying external stress. Additionally, the plastic shape change in load-biased heating–cooling experiments can be decreased with the formation of these precipitates as mentioned before in the literature. However, the main objective of this study was to investigate the aging effect on the functional fatigue behavior for high number of cycles and the fatigue life of $Ni_{50.3}Ti_{29.7}Hf_{20}$ alloy. Here are the conclusions that can be drawn from this study:

(i) The extruded sample lost all its shape memory behavior after 5000 cycles such that the fatigue experiment was ceased. On the other hand, aged sample fractured at 16,534th cycle in the first experiment and showed 1.7% of actuation strain even before the fracture.
(ii) The fatigue life of $Ni_{50.3}Ti_{29.7}Hf_{20}$ alloy was improved with the aging heat treatment at 550 °C for 3 h for more than 3 times.

(iii) The cyclic stability of the alloy in functional fatigue experiments in terms transformation temperatures and actuation strain was enhanced but not fully maintained with the aging process. Therefore, attention should be paid if the alloys are utilized in the actuator type applications with the necessity of high number of cycles.

(iv) The functional fatigue experiments were conducted twice on the extruded and the aged samples and it was observed that the shape memory properties which are the transformation temperatures and the actuation strain values are repeatable. Hence, it can be concluded that the fatigue life of Ni-rich NiTiHf HTSMAs can be enhanced via aging process.

Acknowledgements This study was supported by the Turkish Aviation Industry under Grant No. DKTM/2015/10.

References

1. Singh K, Sirohi J, Chopra I (2003) An improved shape memory alloy actuator for rotor blade tracking. J Intell Mater Syst Struct 14(12):767–786
2. Strelec JK, Lagoudas DC, Khan MA, Yen J (2003) Design and implementation of a shape memory alloy actuated reconfigurable airfoil. J Intell Mater Syst Struct 14(4–5):257–273
3. Hartl DJ, Lagoudas DC (2007) Aerospace applications of shape memory alloys. J Aerosp Eng 221(4):535–552
4. Sanders B, Crowe R, Garcia E (2004) Defense advanced research projects agency–Smart materials and structures demonstration program overview airfoil. J Intell Mater Syst Struct 15(4):227–233
5. Godard OJ, Lagoudas MZ, Lagoudas DC (2003) Design of space systems using shape memory alloys. Smart Mater Struct 5056:545–558
6. Otsuka K, Ren X (2005) Physical metallurgy of Ti–Ni-based shape memory alloys. Prog Mater Sci 50:511–678
7. Kockar B, Karaman I, Kim JI, Chumlyakov YI, Sharp J, Yu CJM (2008) Thermomechanical cyclic response of an ultrafine-grained NiTi shape memory alloy. Acta Mater 56:3630–3646
8. Kockar B, Karaman I, Kulkarni A, Chumlyakov Y, Kireeva IV (2007) Effect of severe ausforming via equal channel angular extrusion on the shape memory response of a NiTi alloy. J Nucl Mater 361:298–305
9. Ma J, Karaman I, Noebe RD (2010) High temperature shape memory alloys. Int Mater Rev 55(5):257–315
10. Kockar B, Atli KC, Ma J, Haouaoui M, Karaman I, Nagasako M, Kainuma R (2010) Role of severe plastic deformation on the cyclic reversibility of a $Ti_{50.3}Ni_{33.7}Pd_{16}$ high temperature shape memory alloy. Acta Mater 58:6411–6420
11. Santamarta R, Arroyave R, Pons J, Evirgen A, Karaman I, Karaca HE, Noebe RD (2013) TEM study of structural and microstructural characteristics of a precipitate phase in Ni-rich Ni–Ti–Hf and Ni–Ti–Zr shape memory alloys. Acta Mater 61:6191–6206
12. Kockar B, Karaman I, Kim JI, Chumlyakov Y (2006) A method to enhance cyclic reversibility of NiTiHf high temperature shape memory alloys. Scr Mater 54:2203–2208
13. Meng XL, Zheng YF, Wang Z, Zhao LC (2000) Shape memory properties of the $Ti_{36}Ni_{49}Hf_{15}$ high temperature shape memory alloy. Mater Lett 45:128–132
14. Karaca HE, Acar E, Tobe H, Saghaian SM (2014) NiTiHf-based shape memory alloys. Mater Sci Technol 30(13):1530–1544
15. Evirgen A, Karaman I, Santamarta R, Pons J, Noebe RD (2015) Microstructural characterization and shape memory characteristics of the Ni50.3Ti34.7Hf15 shape memory alloy. Acta Mater 83:48–60
16. Meng XL, Cai W, Fu YD, Li QF, Zhang JX, Zhao LC (2008) Shape-memory behaviors in an aged Ni-rich TiNiHf high temperature shape-memory alloy. Intermet 16:698–705
17. Evirgen A, Basner F, Karaman I, Noebe RD, Pons J, Santamarta R (2012) Effect of aging on the martensitic transformation characteristics of a Ni-rich NiTiHf high temperature shape memory alloy. Funct Mater Lett 5(4):1250038
18. Karaca HE, Saghaian SG, Ded G, Tobe H, Basaran B, Maier HJ, Noebe RD, Chumlyakov YI (2013) Effects of nanoprecipitation on the shape memory and material properties of an Ni-rich NiTiHf high temperature shape memory alloy. Acta Mater 61:7422–7431
19. Saghaian SM, Karaca HE, Souri M, Turabi AS, Noebe RD (2016) Tensile shape memory behavior of $Ni_{50.3}Ti_{29.7}Hf_{20}$ high temperature shape memory alloys. Mater Des 101:340–345
20. Bigelow GS, Garg A, Padula SA II, Gaydosh DJ, Noebe RD (2011) Load-biased shape-memory and superelastic properties of a precipitation strengthened high-temperature $Ni_{50.3}Ti_{29.7}Hf_{20}$ alloy. Scr Mater 64:725–728
21. Karakoc O, Hayrettin C, Bass M, Wang SJ, Canadinc C, Mabe HJ, Lagoudas DC, Karaman I (2017) Effects of upper cycle temperature on the actuation fatigue response of NiTiHf high temperature shape memory alloys. Acta Mater 138:185–197
22. Karakoc O, Hayrettin C, Canadinc D, Karaman I (2018) Role of applied stress level on the actuation fatigue behavior of NiTiHf high temperature shape memory alloys. Acta Mater 153:156–168
23. Miyazaki S, Igo Y, Otsuka K (1986) Effect of thermal cycling on the transformation temperatures of Ti-Ni alloys. Acta Metall 34:2045–2051
24. McCormick PG, Liu Y (1994) Thermodynamic analysis of the martensitic transformation in NiTi-II. Effect of transformation cycling. Acta Metall Mater 42:2407–2413